JOURNAL OF MATERIALS SCIENCE **38** (2003) 2971 – 2977

Embrittlement of austempered ductile iron on contact with water—testing under applied potential

L. MASUD, R. MARTÍNEZ, S. SIMISON, R. BOERI
INTEMA, National University of Mar del Plata–CONICET, Juan B. Justo 4302–B7608FDQ, Mar del Plata, Argentina
E-mail: boeri@fi.mdp.edu.ar

Recent reports indicate that austempered ductile iron (ADI) is embrittled on contact with water. This environmentally induced cracking (EIC) phenomenon is not clearly understood. The objective of this investigation is to study the behavior of ADI on tensile testing in aqueous media under controlled electrochemical conditions, aiming to identify whether the embrittlement can be either inhibited or enhanced by stimulating or avoiding the reduction of protons on the sample's surface. The results suggest that the EIC of ADI is not an electrochemical phenomenon, since neither cathodic nor anodic applied potentials have been able to inhibit embrittlement. Local wetting of the tensile sample surface has been used to localise fracture. Early stages of fracture propagation have been shown to take place by cleavage. Later, the fracture mode changes to quasi-cleavage, a much more ductile mechanism, as it grows far from the fracture initiation site.

1. Introduction

Austempered ductile iron (ADI) is a high strength material that is being increasingly used in the fabrication of cast parts for a number of industries, such as rail road, automotive, agricultural and others. ADI combines excellent strength and good ductility with low cost and the ability to produce nearly finished parts through casting. It has been then used to replace parts traditionally made of cast, forged or machined steels of different grades. ADI can be produced in different strength grades, reaching minimum properties ranging from 850 MPa to 1600 MPa of tensile strength, and elongation between 10 and 0 respectively [1].

Shibutani *et al.* [2] and Komatsu *et al.* [3] reported that ADI suffers an unusual embrittlement effect when it is tested in tension with the sample surface in contact with water. Later, Martínez *et al.* [4], obtained similar results in an independent laboratory and on different ADI grades. ADI suffers significant reductions in UTS and elongation, that can reach up to 30% and 70% respectively, when tested in tension. The embrittling effect reverses rapidly when the surface is dried. Impact properties are not affected by contact with water. The effect shows no dependency with the time of exposure to water, acting almost instantaneously.

Martínez *et al.* [4] found that embrittlement also takes place when ADI of various ASTM grades is stressed in contact with other liquids, such as isopropyl alcohol and SAE 30 mineral lubricant oil, the effect being less pronounced than that for water. They also reported that the effect of water is independent of its pH, remaining unchanged when water based solutions of pH ranging from 5.5 to 11.9 are used. This does not support earlier proposals of Shibutani [2].

The fracture surface of the embrittled samples has been examined by Komatsu *et al.* [3] and by Martínez *et al.* [4]. Small regions of cleavage fracture are present in most ADI fracture surfaces, conforming a fracture mechanism called quasi-cleavage. The fracture surfaces of tension samples tested in contact with embrittling liquids show a larger proportion of cleavage facets than the fracture surface of samples tested in air.

The cause of the embrittlement remains unexplained. Shibutani [2] and Komatsu [3] find similarities between the embrittlement of ADI and the behavior of hydrogen embrittled materials, and conclude that this effect is induced by the generation of hydrogen atoms from water on the ductile iron surface under plastic deformation. Hydrogen atoms would then diffuse into the ductile iron matrix, causing the embrittlement. This affirmation was further supported by the results of tension testing in H_2 atmosphere, which caused an embrittlement similar to that caused by water. Nevertheless, the mechanism by which the protons that might reduce at the water/ADI interface would cause an almost instantaneous effect has not been analysed. Furthermore, the little dependency of the phenomena with the time of exposure to water, and its fast reversibility, do not precisely fit the usual characteristics of the hydrogen embrittlement effect.

The embrittlement also affects ductile iron of other microstructures, such as those having martensitic and

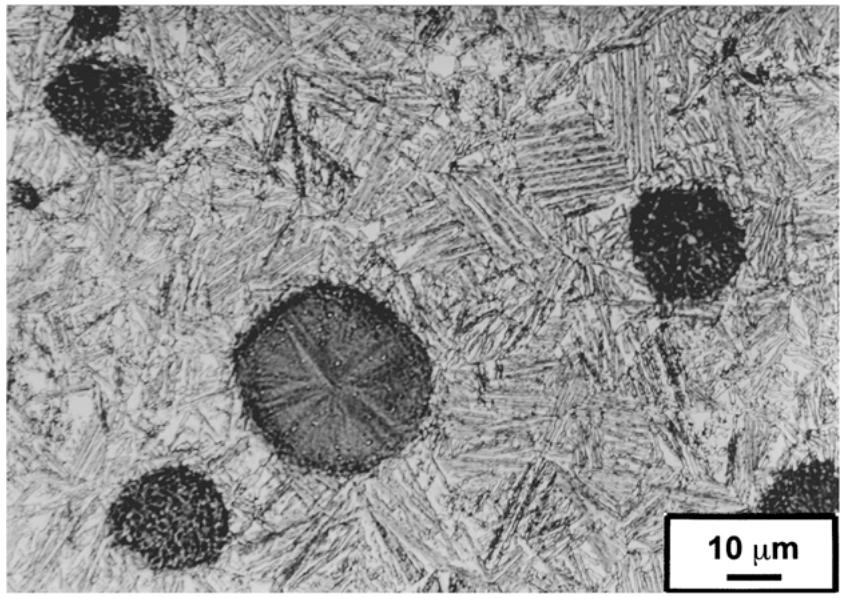

Figure 1 Microstructure of ADI.

pearlitic matrices. Only ferritic matrix ductile iron is immune to the contact with water [2, 3]. A given ductile iron alloy can be heat treated to show ausferritic, martensitic, pearlitic or ferritic matrix. Therefore, the embrittlement mechanism should be primarily related to the microstructure, and not to the chemical composition of the alloy. The solid state transformations during austempering of ADI have been extensively studied [5–9]. The microstructure of ADI is formed of ferrite, austenite and free graphite. Fig. 1 shows the microstructure of ADI austempered at 360°C during 60 min. The black spheroids are the graphite nodules. A fine mixture of ferrite needles and austenite forms the matrix. The austenite is retained at room temperature due to its high content of C.

Martínez *et al.* have discussed the possible role of the different microconstituents on the embrittlement effect. The presence of no individual phase in the microstructure can be considered to be causing the embrittlement [4].

Hydrogen embrittlement (HE), together with stress corrosion cracking (SCC) and liquid metal embrittlement (LME) are the most extensively studied environmentally induced cracking (EIC) processes [10–12]. EIC failures are characterized by brittle failures in which cracks propagate at stress intensity (K) levels lower than the critical values in air or vacuum, as a result of the combined effect of a tensile stress field and the presence of a corrosive media. Corrosion rates are usually quite low. The mechanisms involved in this type of failure are very complex and remain under discussion. In consequence the occurrence of EIC failures in service is still difficult to predict.

HE involves brittle fracture caused by penetration and diffusion of atomic H into the crystal structure of an alloy. Hydrogen can be generated by electrochemical reactions of the type shown in Equations 1 and 2, for neutral and acidic solutions, respectively.

$$H_2O + e^- \rightarrow H + OH^- \quad (1)$$

or

$$H^+ + e^- \rightarrow H \quad (2)$$

A certain time period is required before two H atoms combine on a surface to form a molecule, which depends on the recombination kinetics at the metal surface. The kinetics of the reactions exemplified on Equations 1 and 2 is accelerated by an increase in the cathodic polarization. Thus, cathodic polarisation enhances HE, while anodic polarisation has the opposite effect.

LME causes the catastrophic brittle failure of normally ductile metal alloys when coated by liquid metal and stressed in tension [13]. The fracture mode changes from a ductile to a brittle intergranular or brittle transgranular (cleavage) mode. It has been shown that the stress needed to propagate a sharp crack or a flaw in liquid is significantly lower than that necessary to initiate a crack in the liquid metal environment. In most cases, the initiation and the propagation of cracks appears to occur instantaneously, with the fracture propagating through the entire test specimen. The velocity of crack or fracture propagation has been estimated to be 10 to 100 cm/s.

LME is not a corrosion, dissolution or diffusion–controlled intergranular penetration process. The embrittlement is severe, and the propagation of fracture is very fast in the case of LME as compared to that in SCC.

The objective of this investigation is to study the behavior of ADI on tensile testing in aqueous media under controlled electrochemical conditions, aiming to identify whether the loss of ductility can be either inhibited or enhanced by stimulating or avoiding the reduction of protons on the sample's surface. This study will provide information that should be relevant to clarify the nature of the EIC phenomenon under study. Scanning Electron Microscopy will be used to characterize the fracture surface.

TABLE I Chemical composition of spheroidal graphite cast iron

C	Si	P	Mn	Ni	Cr	Mo	Cu	Mg
3.20	3.30	0.03	0.2	0.68	0.06	0.09	1.00	0.03

2. Experimental methods

The ductile iron melt used was produced in a medium frequency induction furnace by using regular charge materials and standard melting and liquid metal treating practice. The chemical composition is listed on Table I. The melt was cast into one inch Y blocks (ASTM A536-84). Graphite nodules are of size 5, nodularity is 100%, and nodule count is 120 mm^{-2} (ASTM). Tensile test samples of 6.25 mm diameter and 40 mm gauge length (ASTM A370-94) were taken from the prismatic section of the Y blocks.

Ductile iron tensile test samples were austempered to obtain ADI grade 2 (ASTM A 897M-90). The austempering treatment involved an austenitizing stage at 920°C during 60 min, followed by an isothermal stage at 360°C for 60 min in a molten salt bath. Tensile samples were ground down to the final dimensions after heat treatment, to remove all surface material that may have abnormal structure as a result of heat treatment.

The electrochemical behaviour of the ADI samples in water was characterised by recording potenciodynamic polarisation curves. Rotating disk electrodes and a Solartron SI 1280B potentiostat were used. Tests were carried out using a potential sweep rate of 3.10^{-3} V/sec. Static and rotating tests ($\omega = 7$ Hz) were performed. Rotating disk electrodes were assembled as shown in Fig. 2. Working electrodes consisted of 5.9 mm diameter ADI discs mounted on Grilon^{TM} tubes. Samples were tested in a CO_3/HCO_3 buffer solution of pH = 8. Na_2CO_3 (0.1 M) was added as support electrolyte.

The sample surface was polished down to 600 grit SiC paper, rinsed in distilled water, and immersed in the electrolyte solution during 40 min prior to polarisation curves measurement.

Tensile testing of ADI samples in contact with aqueous solutions at controlled potential were carried out using the experimental set-up shown in Fig. 3. A plastic tube with open top and its bottom end closed by a rubber stopper was attached to the calibrated diameter portion of the tensile sample. The tube was filled with the electrolytic solution. A platinum foil of 22 cm^2 surface area was used as counter electrode and a $Cu/CuSO_4$ electrode as reference electrode. The samples were left in contact with the solution until the corrosion potential became stable. Then the specified potential was applied, and the tensile test started. A portable Gamry Instruments Inc. potentiostat was used. The complexity of the set up made impossible the use of extensometers on the sample. The elongation was traced during testing by measuring the displacement of the testing machine head. Fracture elongation was determined by measuring the distance between marks made on the sample surface, before and after testing. All tensile test values reported are the average of three tests and were carried out at strain rate of 0.02 m/m/min.

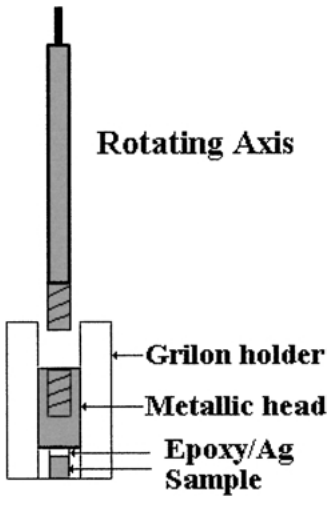

Figure 2 Rotating disk set up.

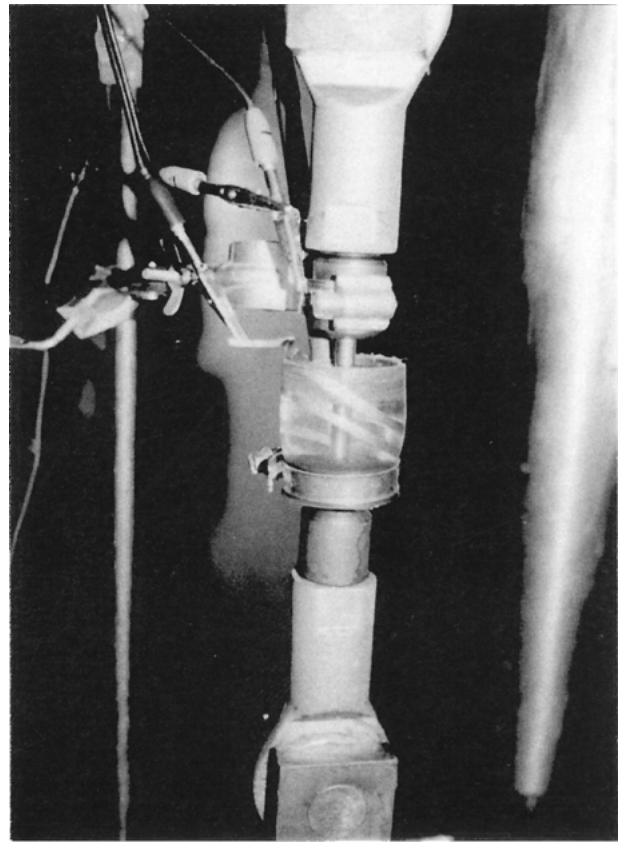

Figure 3 Tensile testing experimetal set-up.

3. Results

3.1. Polarization curves of ADI

Fig. 4 shows potentiodynamic polarization curves with and without sample rotation. The fluid flow affects the cathodic curve and the corrosion potential. The corrosion potential is −0.722+/−0.08 V(SCE) for the stagnant condition, and −0.592+/−0.08 for the rotating condition. As is the case for iron and most steels, the corrosion rate of ADI in neutral or slightly alkaline media is controlled diffusionally by the rate of reduction of dissolved oxygen, and this increases with flow rate.

3.2. Constant potential tensile tests

The values of controlled potential to be applied during tensile testing were chosen based on the results of the

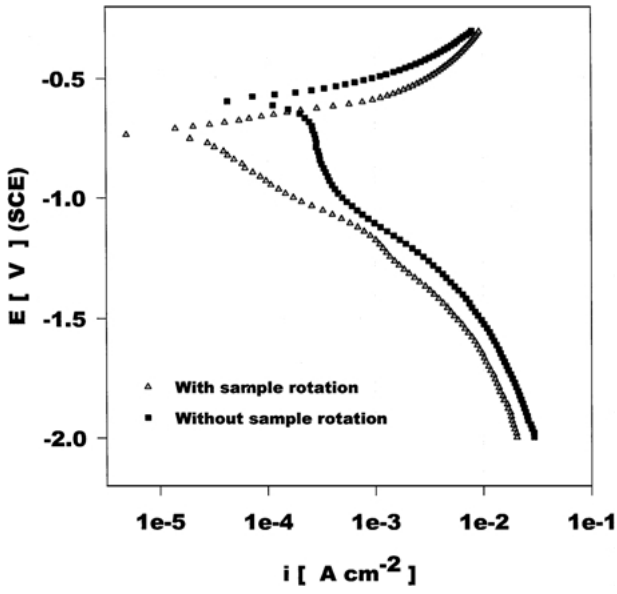

Figure 4 Potentiodynamic polarization curves in $CO_3^{=}/HCO_3^{-}$ buffer solution of pH = 8 (v = 3.10^{-3} V s^{-1}; ω = 7 Hz).

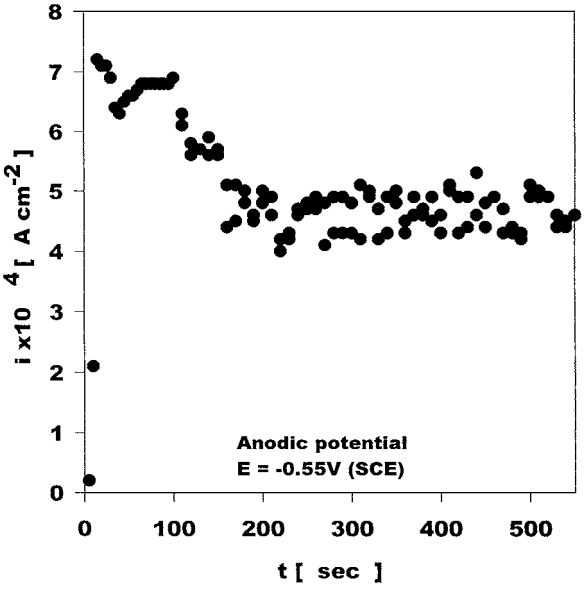

Figure 5 Evolution of current during tensile testing at cathodic potential in $CO_3^{=}/HCO_3^{-}$ buffer solution of pH = 8.

polarisation tests. A potential of −1.45 V (SCE) was used to induce cathodic conditions, in which the generation of hydrogen on the surface is stimulated, and a potential of −0.55 V (SCE) was used to inhibit hydrogen generation.

The results of tensile tests are listed in Table II. Dry testing results are included for comparison. The magnitude of the embrittlement effect caused by water is not affected by the application of anodic or cathodic potential. The evolution of the current during testing for both potentials is shown in Figs 5 and 6. Fig. 6 shows that under anodic potential, after an initial transient, the current falls to a plateau, which indicates that corrosion is generalised. This was confirmed later by the observation of the lateral surfaces of the sample, which showed no signs of localised corrosion.

Even though the results on the effect of applied potential on EIC of ADI are quite conclusive, there was still the need to ascertain that embrittlement has not been caused by an amount of hydrogen generated during the time elapsed from sample immersion to the stabilization of the corrosion potential. Therefore a modified testing methodology was devised. Samples were polarized to the selected anodic potential before the cell was filled with the electrolyte. The results are coincident with those shown in Table II, and therefore no difference in the degree of embrittlement was found.

3.3. Fracture surface characterization

It has been reported that the fracture surface of samples tested in water show some portions of flatter and brighter aspect, characterised by large portions of cleavage fracture mechanism [2–4]. Nevertheless, these regions of the fracture have not been clearly linked to the fracture initiation. In an attempt to localise the initiation of the fracture, the tensile sample surface was put in contact with water only at a very small location, by using a cotton swab previously wet with test solution. This was done during the tensile test at constant load, at a stress level higher than the tensile strength in contact with aqueous solution, but lower than the dry tensile strength. Under this stress condition, contact of the wet cotton swab with the sample surface caused its immediate fracture. Fig. 7 shows a macrography of the fracture surface. The arrow points the location at which the sample surface has been wet. A nearly round, bright and flat fracture area, of approximately 1 mm diameter, appears to originate from such location. The examination of the fracture surface by scanning electron microscopy shows that the fracture mechanism characteristic of the flat regions is cleavage, as shown in Figs 8 and 9. The

TABLE II Results of tensile tests

Test condition	σ_R (Mpa)	Elongation (%)
E_{corr} = −0.69/−0.72 V (SCE)	863	3 (±1)
Cathodic potential = −1.45 V (SCE)	857	3 (±1)
Anodic potential = −0.55 V (SCE)	868	3 (±1)
Dry test	1168	16 (±1)

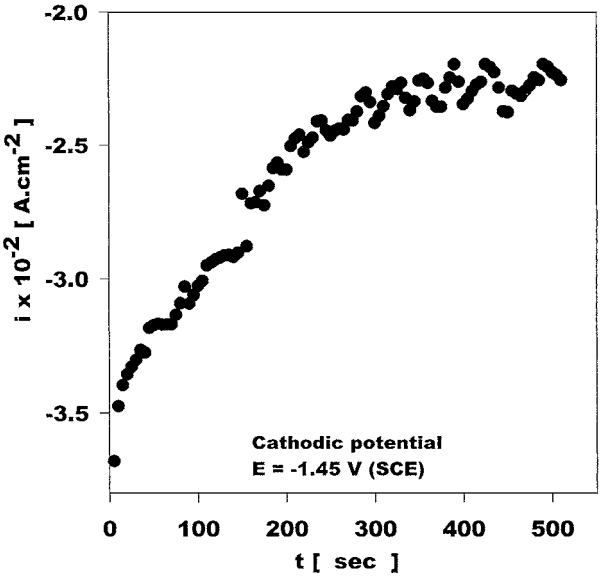

Figure 6 Evolution of current during tensile testing at anodic potential in $CO_3^{=}/HCO_3^{-}$ buffer solution of pH = 8.

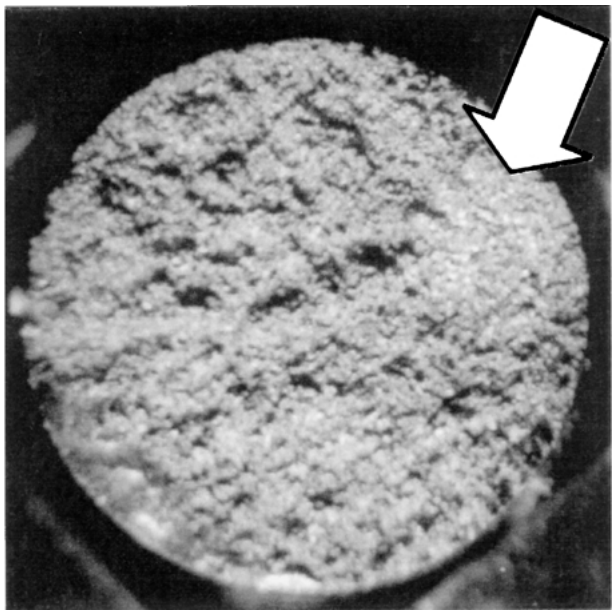

Figure 7 Macrography of the fracture surface.

fracture surface shows graphite nodules and spherical holes left by nodules that remained on the opposite surface. The fracture surface beyond the flat portion, shown in Fig. 10, displays a predominantly ductile fracture, characterised by dimples. Nevertheless, some small areas of cleavage are also present, conforming a fracture type commonly referred to as quasi-cleavage, as that typically found in samples tested in air. The marked difference in the brittleness of both fracture types is also emphasised by the extent of plastic deformation around the graphite nodules, which is much greater on the quasi-cleavage fracture.

The results show that water induces brittle cleavage fracture of ADI. It is also suggested that when flat brittle portions are observed on the fracture surface of tensile samples tested in contact with water, they show the location of the fracture initiation.

4. Discussion

The results suggest that the EIC of ADI is not an electrochemical phenomenon, since neither cathodic

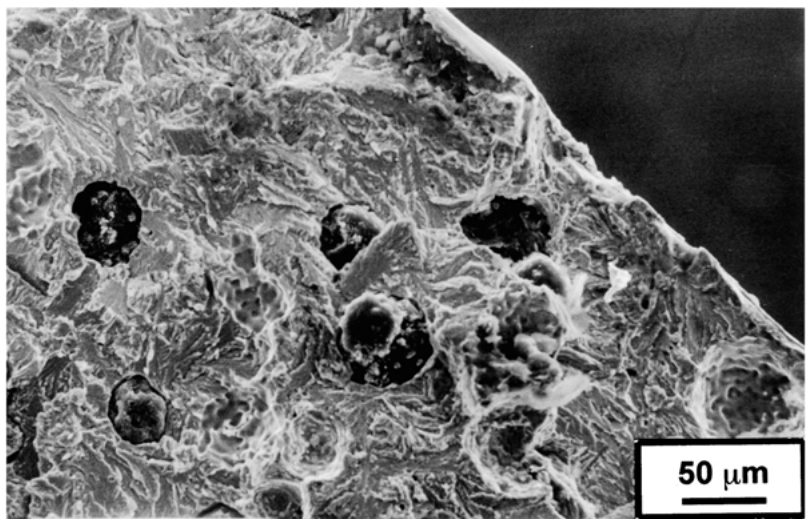

Figure 8 Fracture surface at the flat region pointed in Fig. 7, showing cleavage fracture.

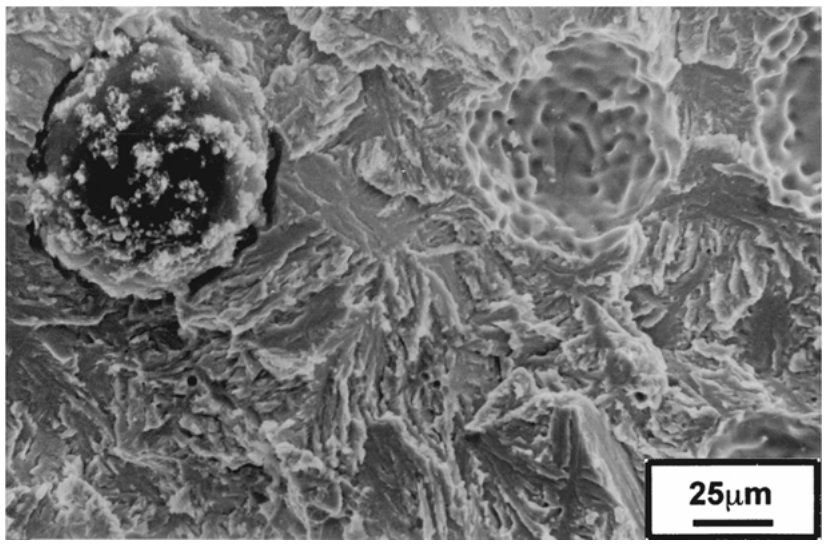

Figure 9 Same region as that shown in Fig. 8, at higher magnification.

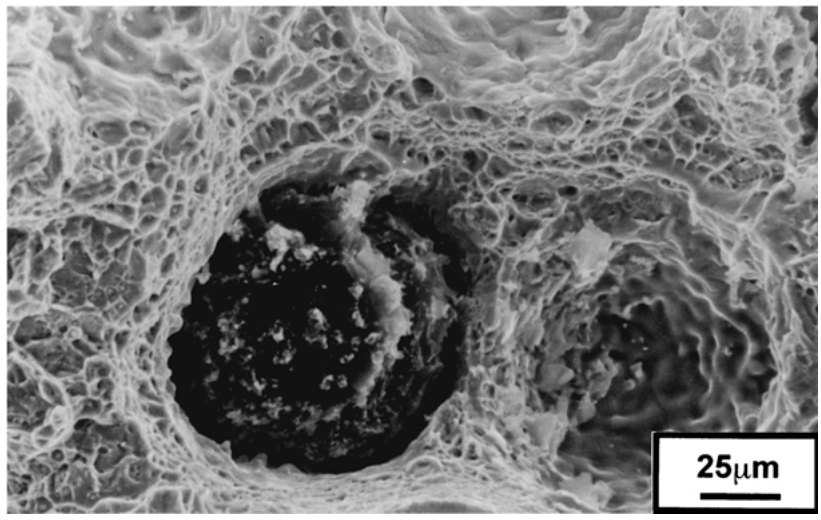

Figure 10 Fracture surface out from the flat region, showing quasi-cleavage fracture mode.

nor anodic applied potentials have been able to inhibit embrittlement. The contact of ADI with water when stressed at tension levels above yielding, causes an instantaneous embrittlement and subsequent fracture. The characteristics of this effect are quite unique, showing no complete similarity with any other EIC reported for metals. The velocity of the process and its fast reversibility resembles LME.

It is proposed that the fracture of ductile iron in contact with water proceeds as follows: upon contact with water, the A—A atomic bonds at an unidentified defect or crack present on the surface of ADI are weakened by the chemisorption of an atom or molecule B, as shown schematically in Fig. 11. The chemisorption process presumably occurs spontaneously or only after the A—A bonds have been strained to some critical value. In any event, electronic rearrangement occurs because of adsorption, which weakens the bonds at the crack tip. When the applied remote stress is increased so that local stress at the crack tip exceeds the reduced breaking strength of A—A bonds, then the crack becomes unstable and grows rapidly [13, 14]. The crack grows initially in a brittle manner, by cleavage, but changes to quasi-cleavage, a much more ductile mechanism, as it grows far from the fracture initiation site. For the present load conditions, stress levels and sample dimensions, for the K_{1C} value of 90 MPa $m^{1/2}$, the critical defect size can be estimated to be 0.8 mm [15]. This would indicate that if the presence of water activates the rapid growth of a crack, and such crack extends beyond the critical defect size, then, even when the fracture mode changes to a higher energy consuming mechanism, the remaining ligament will not be able to stop fracture, and the sample will collapse. The size of the cleavage fracture surface was approximately 1 mm in the present experiments, which is slightly larger than the calculated dimension of the critical defect, and supports the proposed mechanism.

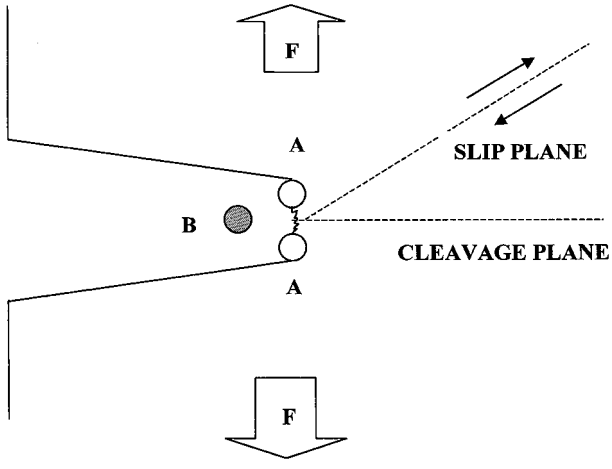

Figure 11 Schematic representation of the proposed embrittlement mechanism.

The independence of the EIC of ADI from the reduction of protons at the sample surface does not initially support that H atoms are responsible for the embrittlement. The participation of H atoms is also doubtful, considering that other liquids have also shown to cause EIC of these alloys [4].

Future work should continue to be focused on the clarification of the mechanism of EIC responsible for the embrittlement of ADI. In particular, it is necessary to identify the role of surface energy on fracture, and to recognise fracture initiation sites at the sample surface, at a microscopic level.

5. Conclusions

- The application of controlled potential during tensile testing of ADI in contact with water neither enhances nor inhibits the embrittlement effect observed under free potential testing conditions. This has been the case for both anodic and cathodic conditions.
- The independence of the extent of the environmentally induced cracking of ADI from the reduction of protons at the sample surface does not support that H atoms are responsible for the embrittlement, and indicates that fracture of ADI in contact with water is not an electrochemical phenomenon.
- The use of local wetting of the tensile sample surface caused localised fracture. Early stages of fracture propagation take place by cleavage. Later, fracture

mode changes to quasi-cleavage, a much more ductile mechanism typical of dry fracture, as it grows far from the fracture initiation site.

Acknowledgement

This research was supported by a grant from the National University of Mar del Plata, Argentina.

References

1. ASTM A 897M-90. "Standard Specification for Austempered Ductile Iron Castings," Annual Book of ASTM Standards, Philadelphia, 1995.
2. S. SHIBUTANI, S. KOMATSU and Y. TANAKA, *Int. J. Cast. Metals Research*, **11**(6) (1999) 579.
3. S. KOMATSU, C. ZHOU, S. SHIBUTANI and Y. TANAKA, *ibid.* **11**(6) (1999) 579.
4. R. A. MARTÍNEZ, R. BOERI and J. A. SIKORA, *ibid.* **14**(3) (2000) 9.
5. R. ELLIOT, "Cast Iron Technology" (Butterworths & Co. Ltd. London, 1988).
6. R. GUNDLACH and J. JANOWAK, in Proceedings of the First World Conference on ADI-Rosemont (Chicago), Illinois April, 1984 (1994) p. 1.
7. T. N. ROUNS and K. B. RUNDMAN, *Trans. Amer. Found. Soc.* **95** (1987) 851.
8. N. DARWISH and R. ELLIOTT, *Mater. Sci. and Technol.* **9** (1993) 586.
9. J. SIKORA and R. BOERI, *Int. J. Cast Metals Research* **11**(6) (1999) 395.
10. D. A. JONES, "Principles and Prevention of Corrosion," 2nd ed. (Macmillan Publ. Company, New York, 1995).
11. R. W. HERTZBERG, "Deformation and Fracture Mechanics of Engineering Materials," 3rd ed. (Wiley, Singapore, 1989).
12. J. R. GALVELE, *Corrosion* **8** (1999) 723.
13. "ASM Handbook," Vol. 13, 9th ed. (ASM International, 1992).
14. M. H. KAMDAR, *Progr. Mater. Sci.* **15** (1973) 289.
15. "Stress Intensity Factors Handbook," edited by Y. Murakami (The Society of Materials Science, Japan, Pergamonn Press, 1990).

Received 10 January 2002
and accepted 17 April 2003